5838–5842 Nucleic Acids Research, 1993, Vol. 21, No. 25

An 'elaborated' pseudoknot is required for high frequency frameshifting during translation of HCV 229E polymerase mRNA

J.Herold and S.G.Siddell
Institute of Virology, University of Würzburg, Versbacher Straße 7, 97078 Würzburg, Germany

Received October 4, 1993; Revised and Accepted November 22, 1993 EMBL accession no. X69721

ABSTRACT

The RNA polymerase gene (gene 1) of the human coronavirus 229E is approximately 20 kb in length and is located at the 5′ end of the positive-strand genomic RNA. The coding sequence of gene 1 is divided into two large open reading frames, ORF1a and ORF1b, that overlap by 43 nucleotides. In the region of the ORF1a/ORF1b overlap, the genomic RNA displays two elements that are known to mediate (−1) ribosomal frameshifting. These are the slippery sequence, UUUAAAC, and a 3′ pseudoknot structure. By introducing site-specific mutations into synthetic mRNAs, we have analysed the predicted structure of the HCV 229E pseudoknot and shown that besides the well-known stem structures, S1 and S2, a third stem structure, S3, is required for a high frequency of frameshifting. The requirement for an S3 stem is independent of the length of loop 2.

INTRODUCTION

Expression of the RNA-dependent replicases of a variety of viruses involves ribosomal frameshifting during translation. For example, retroviruses (1, 2, 3), yeast double-stranded RNA virus (4), luteoviruses (5, 6), toroviruses (7), arteriviruses (8) and coronaviruses (9, 10, 11, 12) use this strategy. The signal responsible for frameshifting commonly consists of a slippery sequence containing two homopolymeric triplets, often followed by a stable tertiary RNA structure, a hairpin or a pseudoknot (13).

The slippery sequence is the site where frameshifting takes place. This has been shown by amino acid sequencing of the Rous Sarcoma Virus (RSV) *gag-pol* and the human T-cell leukemia virus type I (HTLV-I) *gag-pro* transframe proteins (14, 15). Jacks and colleagues have proposed a 'simultaneous slippage model' in which a ribosome slips back into the (−1) reading frame of the mRNA at the last codon of the slippery sequence. Translocation then takes place and further decoding of the mRNA continues (14).

Although the sequences of slippage sites differ, they always allow a stable interaction of the tRNAs with the mRNA in both the A- and P-site after the frameshifting event (16). Brierley and colleagues (17) have performed a detailed mutational analysis of the slippery sequence of IBV, a coronavirus, and deduced that the frequency of frameshifting is largely dependent upon the strength of the tRNA interaction with the A site codon in the zero reading frame of the slippery sequence.

A computer aided analysis of the sequences around proven or putative frameshift sites in a number of viral RNAs, led to the conclusion that a stable tertiary structure is also necessary for high frequency ribosomal frameshifting (13). In almost all cases, a stable hairpin or a pseudoknot structure has been predicted to form downstream of the potential slippage site. H-type pseudoknots consist of a stem-loop structure where bases in the loop are able to pair with bases outside the hairpin (18, 19). The two stems of the pseudoknot are thought to form a stacked, quasi-continuous double helix connected by two loops (20). Destabilization of the hairpin or the pseudoknot by site directed mutagenesis has been shown to reduce or even abolish frameshifting (6, 14, 21).

The exact mechanism of the shifting event is still unsolved, but it is thought that ribosomal pausing caused by the stable RNA structure is a prerequisite for frameshifting (14, 17). Heelprinting experiments on *Saccharomyces cerevisiae* virus RNA provides evidence that ribosomes have a decreased rate of movement through a pseudoknot and that paused ribosomes are located directly over the slippery sequence (22).

We have recently sequenced the RNA polymerase gene of the human coronavirus HCV 229E (12, EMBL/GenBank/DDBJ X69721). This gene is composed of two open reading frames, ORF1a and ORF1b, that overlap by 43 nucleotides. RNA encompassing this overlap region was able to mediate a high frequency (20–30%) of frameshifting in a reticulocyte lysate (12). In the overlap region, we were able to identify a slippery sequence, UUUAAAC, and a potential downstream H-type pseudoknot. However, the pseudoknot we predicted had an S2 stem of only 5 base-pairs and an unusually large loop of 166 nucleotides connecting the S1 and S2 stems. In this paper, we report a mutational analysis that confirms the predicted pseudoknot structure and, at the same time, reveals a third stem structure, S3, that is required for high frequency frameshifting.

MATERIALS AND METHODS

Construction of plasmid pFS 1

A 1,264 base-pair *NdeI*−*HpaI* cDNA fragment corresponding to nucleotides (nt.) 12,293−13,557 in the HCV 229E genome and including the putative HCV 229E frameshifting components was treated with the Klenow fragment of DNA polymerase and exchanged with the small (230 base-pair) *Eco*RV fragment of pSP65-GUS (6, 12). A clone containing the HCV 229E DNA fragment in the correct orientation, pFS 1, was identified by restriction enzyme analysis and the construction was verified by sequencing.

Site-specific mutagenesis

Mutations within the HCV 229E pseudoknot structure were introduced by an *in vivo* recombination-PCR method (23). Four partially complementary oligonucleotides, two of them carrying the desired mutation, were used to generate linear fragments of plasmid DNA. These fragments were combined without further purification and used to transform *E.coli* TG-1 cells. Recombination in vivo of the linear products effected the generation of circular plasmids carrying the desired mutation. The introduced mutations were verified by double-stranded sequencing.

In vitro transcription and translation

Plasmid DNA was linearized with *Bst*EII and transcribed with SP6 RNA polymerase as described (12, 24). The *in vitro* synthesized, capped RNAs were translated in a rabbit reticulocyte lysate (Promega) in the presence of ^{35}S-methionine and the products were analysed on 10% polyacrylamide-SDS gels as described previously (25). The radioactivity incorporated into the translation products was determined using a PhosphorImager Model 400E (Molecular Dynamics, Sunnyvale, USA)

RESULTS

We have shown previously that HCV 229E gene 1 mRNA contains an element capable of mediating a high frequency (20−30%) of ribosomal frameshifting (12). We predicted that this element was composed of a slippery sequence and an H-type pseudoknot with the following co-ordinates; SH, nt.12514−12520; SP, nt.12521−12525; S1, nt.12526−12537 plus 12546−12557; L1, nt.12538−12540; HL, nt.12526−12557; S2, nt.12541−12545 plus 12723−12727; L2, nt.12558−12722 (12, figure 1, for terminology see 13). This prediction was based upon analogy to other frameshifting elements, computer-assisted modelling and the loss of frameshifting activity in a synthetic mRNA containing a deletion that encompassed the 3′ component of the predicted S2 stem (12).

To confirm the proposed model and to determine the importance of defined base-pairs for the functional integrity of the pseudoknot, we derived a panel of synthetic mRNAs with mutations predicted to destabilize specific base-paired regions of the structure. As a control, we also derived mRNAs with complementary mutations predicted to restabilize these regions, although with a different RNA sequence. The frameshifting activities of the mutated mRNAs were then tested *in vitro*.

Base-pairing in stem 1 is necessary for ribosomal frame shifting

As expected, mutations that destablized base-pairs involved in stem 1 of the predicted pseudoknot dramatically reduced frameshifting activity. mRNA derived from pFS 1 mut 18, in which four potential base-pairs in stem 1 were destabilized, had no detectable activity. We estimate the sensitivity of the PhosporImager analysis to be about 1 % of the 'wild-type' level (i.e., an absolute frameshifting frequency of 0.2−0.3%) and suggest, therefore, that base-pairing in stem 1 is necessary for a significant level of ribosomal frameshifting in this system. Compensating mutations that restored the same stem 1 base-pairs with a different sequence (pFS1 mut 17) resulted in a mRNA with the 'wild-type' levels of frameshifting activity (figure 2).

Base-pairing in stem 2 is necessary for a high level of ribosomal frameshifting

In the predicted HCV 229E pseudoknot, stem 2 is composed of only 5 base-pairs. Destabilization of the central base-pair (pFS

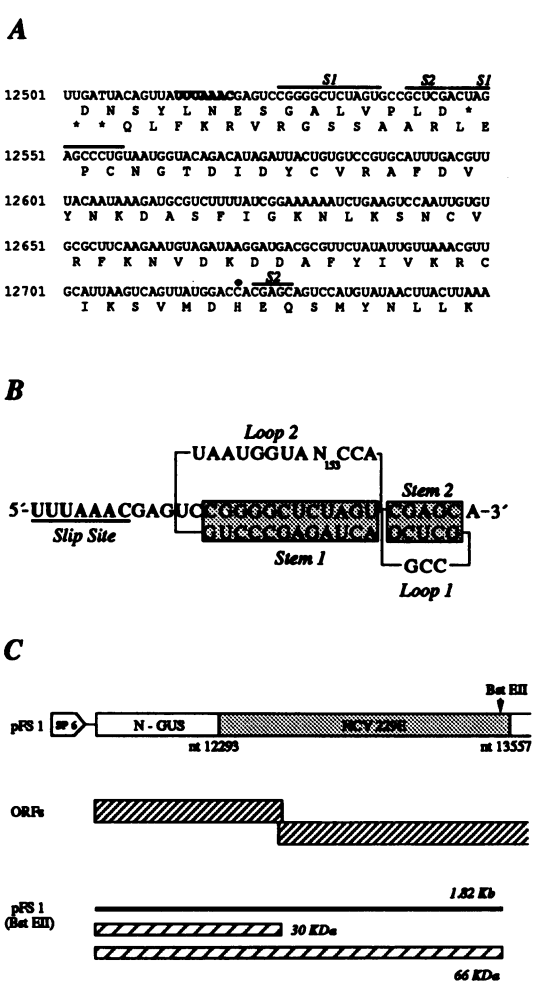

Figure 1. A. The sequence of the region encompassing the HCV 229E frameshifting element. The putative slippage site, the nucleotides predicted to be involved in the H-type pseudoknot and the amino acid sequence of ORFs 1a and 1b, at their C and N termini respectively, are shown. The nucleotide numbering corresponds to the HCV 229E genomic sequence and the point (·) indicates the 3′ limit of the HCV 229E sequences in pΔFS (12). **B.** A schematic representation of the predicted (12) HCV 229E frameshifting element, inculding the slippery sequence and an H-type pseudoknot. **C.** The structure of the plasmid pFS 1 and the *in vitro* translation products of pFS 1/BstEII run-off mRNA. The DNA structure of pFS 1 is schematically shown together with the position of the HCV 229E ORF1a/ORF1b overlap. The size of the SP6 run-off transcription product and the translation products predicted in the event of ORF1a termination or (−1) ribosomal frameshifting are shown.

1 mut 16 or pFS 1 mut 2) reduced the frameshifting activity of the corresponding mRNA to approximately 10% of the 'wild-type' level. Replacing the central base-pair with an energetically neutral U-G base-pair decreased the frameshifting activity, but only by 20% (pFS 1 mut 1). Restoration of the central base-pair in the reverse orientation (pFS 1 mut 25) resulted in a mRNA with higher than normal frameshifting activity (figure 2). These results show that base-pairing in the predicted S2 stem is required for a high level of frameshifting. The mutations introduced in pFS 1 mut 2 or pFS 1 mut 16 RNA did not result in a complete loss of frame shifting activity. However, it is possible that the introduction of further destabilizing mutations in this region would reduce the frameshifting activity to a lower level.

Base-pairing outside the S1 and S2 stems is necessary for a high level of ribosomal frameshifting

A computer-assisted analysis of possible base-pairing interactions in the region of the HCV 229E pseudoknot led us to the recognition of a putative stem structure, S3, which involved base-pairing on either side of the 3′ component of stem 2. A similar complex structure has also been proposed by Tang and Draper in the leader of the a operon mRNA of *E.coli* where it is recognized by a translational repressor protein (26). To investigate whether this structure has a functional role in the frameshifting activity of the HCV 229E pseudoknot, we introduced destabilizing mutations in the core of the putative stem 3 duplex (pFS 1 mut 7 and pFS 1 mut 3). mRNAs derived from these plasmids had 10% or less of the 'wild-type' frameshifting activity. Compensatory mutations (pFS 1 mut 9 and pFS 1 mut 4, respectively) restored the activity, although not completely. Destabilizing mutations at the distal end of the predicted S3 stem (i.e., distal to nucleotides involved in the S2 stem) did not significantly reduce frameshifting activity (pFS 1 mut 11). Mutations beyond the predicted S3 stem (pFS 1 mut 27) also had no effect (figure 2). Taken together, these results suggest that nt.12714−12720 together with nt.12729−12735, which

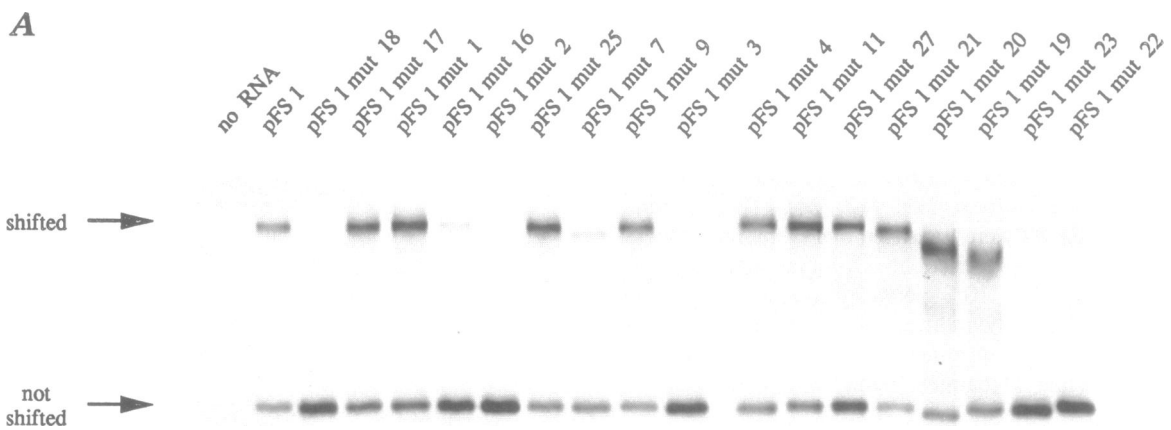

B

Plasmid	RNA - Sequence																Rel. Frameshifting
	SH	SP	5′-S1	L1	5′-S2	3′-S1	L2			5′-S3	L3	3′-S2	[L4]	3′-S3			
pFS 1	UUUAAAC	GAGUC	CGGGGCUCUAGU	GCC	GCUCG	ACUAGAGCCCUG	UAA	148 nts	CAGU	UAUGGAC	CA	CGAGC	A	GUCCAUG	UAUA		1
pFS 1 mut 18	-------	-----	----CGAG---	---	-----	----------	---	...	----	-------	--	-----	-	-------	----		0
pFS 1 mut 17	-------	-----	----CGAG---	---	-----	----CUCG---	---	...	----	-------	--	-----	-	-------	----		1
pFS 1 mut 1	-------	-----	----------	---	-----	----------	---	...	----	-------	--	--G--	-	-------	----		0.8
pFS 1 mut 16	-------	-----	----------	---	--A--	----------	---	...	----	-------	--	--G--	-	-------	----		< 0.1
pFS 1 mut 2	-------	-----	----------	---	-----	----------	---	...	----	-------	--	--U--	-	-------	----		< 0.1
pFS 1 mut 25	-------	-----	----------	---	--A--	----------	---	...	----	-------	--	--U--	-	-------	----		1.3
pFS 1 mut 7	-------	-----	----------	---	-----	----------	---	...	----	-----UG	--	-----	-	CC-----	----		0.1
pFS 1 mut 9	-------	-----	----------	---	-----	----------	---	...	----	-----UG	--	-----	-	CA-----	----		0.9
pFS 1 mut 3	-------	-----	----------	---	-----	----------	---	...	----	-------	--	-----	-	--AGG--	----		< 0.1
pFS 1 mut 4	-------	-----	----------	---	-----	----------	---	...	----	---CCU-	--	-----	-	--AGG--	----		0.7
pFS 1 mut 11	-------	-----	----------	---	-----	----------	---	...	----	--G----	--	-----	-	----- CC	----		0.8
pFS 1 mut 27	-------	-----	----------	---	-----	----------	---	...	--CC	-------	--	-----	-	-------	AU--		1
pFS 1 mut 21	-------	-----	----------	---	-----	----------	---	110 nts	----	-------	--	-----	-	-------	----		1
pFS 1 mut 20	-------	-----	----------	---	-----	----------	---	50 nts	----	-------	--	-----	-	-------	----		1.1
pFS 1 mut 19	-------	-----	----------	---	-----	----------	---	11 nts	----	-------	--	-----	-	-------	----		0.8
pFS 1 mut 23	-------	-----	----------	---	-----	----------	---	110 nts	----	-------	--	-----	-	--AGG--	----		< 0.1
pFS 1 mut 22	-------	-----	----------	---	-----	----------	---	50 nts	----	--------	--	-----	-	--AGG--	----		< 0.1

Figure 2. A. *In vitro* translation of mRNAs derived from pFS 1 and pFS 1 mutant plasmids. Plasmid DNA was linearized with BstEII, transcribed and translated as described in Materials and Methods and the terminated and transframe proteins,separated on a 10% polyacrylamide SDS-gel, were visualised by autoradiography. **B.** Sequence and frameshifting activities of mRNAs derived from pFS 1 and pFS 1 mut plasmids. The mutations introduced in the pFS 1 mut plasmids are shown as transcribed RNA in the context of the 'elaborated' pseudoknot model shown in figure 3. The incorporation of radioactivity into the terminated and transframe translation products shown in A was quantitated by Phosphor Imager analysis and the frequency of frameshifting was calculated (terminated product, 5 methionines; transframe product 19 methionines). The frameshifting frequencies are normalised to mRNA derived from pFS 1.

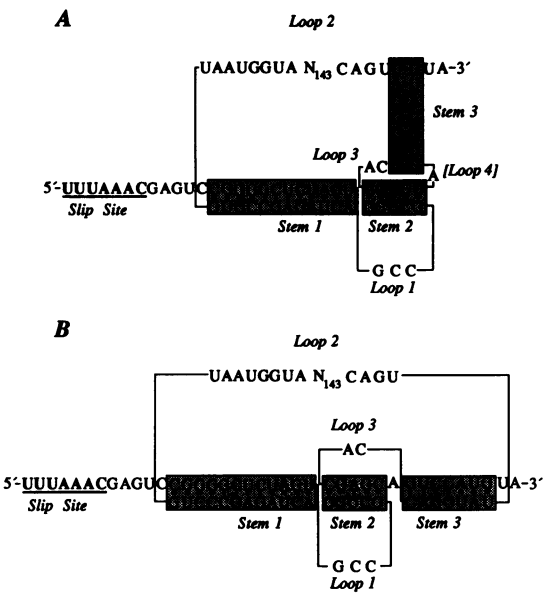

Figure 3. A model of the HCV 229E frameshifting element including the slippery sequence and an 'elaborated' pseudoknot structure. Base-pairs which have been analysed in this study (|) are distinguished from those predicted by modelling (·). **A.** Stem 3 forms a branch from the stem 1/2 axis. **B.** Stem 3 stacks onto, and elongates the quasi-continuous helix of stems 1 and 2.

flank the 3′ component of stem 2, form a stable structure that has an important functional significance for the frameshifting activity of the HCV 229E pseudoknot.

A shorter loop 2 has no influence on the level of ribosomal frameshifting

Although there is theoretically no upper limit for the length of loop 2 in an H-type pseudoknot (18), it has been shown for the IBV pseudoknot that an insertion of 467 nt. at this position dramatically decreases the level of ribosomal frameshifting (21). To investigate if a shorter loop 2 in the HCV 229E pseudoknot influences the level of frameshifting, we shortened loop 2 (which we now define as the distance from the 3′ end of stem 1 to the 5′ end of stem 3) from 157 nt. to 119 nt. (pFS 1 mut 21), 59 nt. (pFS 1 mut 20) or 20 nt. (pFS 1 mut 19). We could detect no significant differences in the ability of the mutant RNAs to direct ribosomal frameshifting compared to the 'wild-type' sequence (figure 2).

A shorter loop 2 cannot compensate mutations in stem 3

Since an unusually long loop 2 as well as a stem 3 structure seems to be a unique feature of the HCV 229E pseudoknot, we investigated whether a 'non-elaborated' pseudoknot (i.e., a pseudoknot with a shorter loop 2 and lacking a potential stem 3) would be able to mediate a high level of ribosomal frameshifting. Using the *in vivo* recombination system we shortened loop 2 of pFS 1 mut 3 from 157 nt to 119 nt. (pFS 1 mut 23) or 59 nt.(pFS 1 mut 22). We could not detect any change in the level of frameshifting, i.e. less than 10% of 'wild-type', indicating that base-pairing in stem 3 is necessary for a fully functional pseudoknot irrespective of the length of loop 2 (figure 2).

DISCUSSION

The results presented here confirm and extend our model of the HCV 229E gene 1 mRNA frameshifting element (12). The sequence UUUAAAC that is found at position 12,514−12,520 in the genomic sequence, 27 bases upstream of the ORF1a termination codon, is almost certainly the HCV slippery sequence. It is identical to the slippage site of IBV (17) and the putative slippage sites of the murine coronaviruses, MHV-JHM (11) and MHV-A59 (10), as well as the closely related Berne Virus (7). Mutations at this site also obviate the frameshifting activity of synthetic HCV 229E mRNAs (Herold, unpublished data). The second component of the frameshifting element is a pseudoknot, located downstream of the slippage site. Our results indicate that the HCV 229E pseudoknot is composed of at least three functionally important regions of double-stranded RNA, S1, S2 and S3.

Analysis of the frameshifting activity of mRNA derived from pFS 1 mut 18 suggests that the S1 stem structure is essential for a functional HCV 229E pseudoknot, as has also been shown in the IBV system (21). Recently Reil and colleagues (27) presented data indicating that the human immunodeficiency virus type 1 (HIV-1) heptanucleotide sequence, UUUUUUA, is sufficient to mediate ribosomal frameshifting n mammalian cell lines at levels of 0.4−0.7%. This level of frameshifting is close to the estimated sensitivity of our assay, so we cannot exclude a basal level of frameshifting activity in pFS 1 mut 18 derived RNA. However, in the context of HCV 229E replication, we would predict a strong selection against this type of mutation.

All mutations predicted to destabilize the RNA duplex of S2 led to decreased but detectable levels of frameshifting in our experiments. One possible interpretation of this data is that the HCV 229E slippery sequence, together with stem 1, is able to mediate ribosomal frameshifting at a low level but that stem 2 acts as a positive modulator. However, we recognize that further experiments are needed to determine whether stem 2 has an obligatory or a modulatory role in the frameshifting activity of the pseudoknot. At the moment, there is no information on the ratio of pol1a and pol1a-pol1b gene products synthesised in coronavirus infected cells or the importance of this stoichiometry in the virus replication cycle. In a number of systems, including HIV (28), potato leafroll virus (6) or the *E.coli* dnaX gene (29), a low level of frameshifting appears to produce sufficient transframe protein, whereas in others, such as coronaviruses, a high level of frameshifting appears to offer a selective advantage.

Finally, the analysis of mRNAs derived from pFS 1 mut 7, 3, 9, 4, 11 and 27 indicated that a third stem structure, S3, is a necessary component of the HCV 229E pseudoknot. This structure has not been previously recognized and we suggest that it may define a special class of frameshifting pseudoknot. Two alternative models which incorporate stem 3 into the pseudoknot structure can be proposed. In the first model, stem 3 forms a branch from the stem 1/stem 2 axis. In the second model, stem 3 stacks onto, and elongates, the quasi-continuous helix of stems 1 and 2 to a length of 24 base pairs (figures 3A and 3B). In the second model, which we prefer, the two unpaired nucleotides that form loop 3 would have to cross the deep major groove of stem 2 parallel to the three unpaired nucleotides of loop 1. Two nucleotides are theoretically sufficient to bridge the five base pairs of stem 2 (18). The unpaired A nucleotide at position 12 728 would lie between stem 3 and stems 1 and 2. However, NMR

analysis of the mouse mammary tumor virus pseudoknot (30) indicates that a single unpaired nucleotide between two adjacent stems does not disturb stacking to a quasi-continuous helix.

Clearly, direct structural analysis will be required to distinguish between the models described above. Nevertheless, the consequence of a third stem in the HCV 229E pseudoknot structure will be to increase the thermodynamic stability of the element and, we predict, to prolong the time ribosomes pause at the slippery sequence. This in turn, will result in a pseudoknot structure that mediates ribosomal frameshifting at a high frequency.

It is noteworthy that similar 'elaborated' pseudoknots can be modelled for other coronaviruses, such as IBV and MHV (Herold, unpublished). However, in contrast to our data, the experiments of Brierley *et al.* (21) indicate that, at least for the IBV pseudoknot, the putative stem 3 structure is not essential for frameshifting activity. Further experiments are needed to explain this difference.

ACKNOWLEDGEMENTS

We thank Babara Schelle-Prinz for expert technical assistance. This work was supported by the Deutsche Forschungsgemeinschaft (SFB 165/B1).

REFERENCES

1. Jacks,T. and Varmus,H.E. (1985) *Science*, **230**, 1237–1242
2. Moore,R., Dixon,M., Smith,R., Peters,G. and Dickson,C. (1987) *J. Virol.*, **61**, 480–490
3. Chamorro,M., Parkin,N. and Varmus,H.E. (1992) *Proc. Natl. Acad. Sci. USA.*, **89**, 713–717
4. Dinman,J.D., Tateo,I. and Wickner,R.B. (1991) *Proc. Natl. Acad. Sci. USA.*, **88**, 174–178
5. Brault,V. and Miller,W.A. (1992) *Proc. Natl. Acad. Sci. USA*, **89**, 2262–2266
6. Prüfer,D., Tacke,E., Schmitz,J., Kull,B., Kaufmann,A. and Rohde,W. (1992) *EMBO J.*, **11**, 1111–1117.
7. Snijder,E.J., den Boon,J.A., Bredenbeck,P.J., Horzinek, M.C., Rijnbrand,R. and Spaan,W.J.M. (1990) *Nucleic Acids Res.*, **10**, 4535–4540
8. den Boon,J.A., Snijder,E.J., Chirnside,E.D., de Vries, A.A.F., Horzinek,M.C. and Spaan,W.J.M. (1991) *J. Virol.*, **65**, 2910–2920
9. Brierley,I., Boursnell,M.E., Binns,M.M., Bilimoria, B., Blok,V.C., Brown,T.D.K. and Inglis,S.C. (1987) *EMBO J.*, **6**, 3779–3785.
10. Bredenbeek,P.J., Pachuk,C.J., Noten,A.F., Charite,J., Luytjes,W., Weiss,S.R. and Spaan,W.J. (1990) *Nucleic Acids Res.*, **18**, 1825–1832.
11. Lee,H.J., Shieh,C.K., Gorbalenya,A.E., Koonin,E.V., La Monica,M.N., Tuler,J., Bagdzhadzhyan,A. and Lai,M.M.C. (1991) *Virology*, **180**, 567–582.
12. Herold,J., Raabe, T., Schelle-Prinz, B. and Siddell, S.G. (1993) *Virology*, **195**, 681–690
13. ten Dam,E.B., Pleij,C.W.A. and Bosch, L. (1990) *Virus Genes*, **4**, 121–136
14. Jacks,T., Madhani,H.D., Marsiarz,F.R. and Varmus,H.E. (1988) *Cell*, **55**, 447–458
15. Nam,S.H., Copeland,T.D., Hatanaka,M. and Oroszlan,S. (1993) *J. Virol.*, **67**, 196–203
16. Hatfield,D. and Oroszlan,S. (1990) *Trends Biochem. Sci.*, **15**, 186–190
17. Brierley,I., Jenner,A. J. and Inglis,S. C. (1992) *J. Mol. Biol.*, **227**, 463–479.
18. Pleij,C.W.A., Rietveld,K. and Bosch,L. (1985) *Nucleic Acids Res.*, **13**, 1717–1731
19. Pleij,C.W.A. (1990) *Trends Biochem. Sci.*, **15**, 143–147
20. Puglisi,J.D., Wyatt,J.R. and Tinoco,I. (1990) *J. Mol. Biol.*, **214**, 437–453
21. Brierley,I., Rolley,N. J., Jenner,A. J. and Inglis, S. C. (1991) *J. Mol. Biol.*, **220**, 889–902.
22. Tu,C., Tzeng,T.-H. and Bruenn,J.A. (1992) *Proc. Natl. Acad. Sci. USA*, **89**, 8636–8640
23. Yao,Z., Jones,D.H. and Grose,C. (1992) *PCR Methods and Applications*, **1**, 205–207
24. Melton,D.A., Krieg,P.A., Rebagliati,M.R., Maniatis, T., Zinn,K. and Green,M.R. (1984) *Nucleic Acids Res.*, **12**, 7035–7056.
25. Siddell,S. (1983) *J. Gen. Virol.*, **64**, 113–125
26. Tang,C.K. and Draper,D.E. (1989) *Cell*, **57**, 531–536
27. Reil,H., Kollmus,H., Weidle,U.H. and Hauser,H. (1993) *J. Virol.*, **67**, 5579–5584
28. Parkin,N.T., Chamorro,M. and Varmus,H.E. (1992) *J. Virol.*, **66**, 5147–5151
29. Tsuchihashi,Z. (1991) *Nucleic Acids Res.*, **19**, 2457–2462
30. Farabaugh,P.J. (1993) *Cell*, **74**, 591–596